Journal of Applied Physics

Experimental investigation of the predicted band structure modification of Mg_2X (X: Si, Sn) thermoelectric materials due to scandium addition

Cite as: J. Appl. Phys. **125**, 225103 (2019); https://doi.org/10.1063/1.5089720
Submitted: 22 January 2019 . Accepted: 16 May 2019 . Published Online: 11 June 2019

Aryan Sankhla, Mohammad Yasseri, Hasbuna Kamila, Eckhard Mueller, and Johannes de Boor

Journal of Applied Physics ARTICLE scitation.org/journal/jap

Experimental investigation of the predicted band structure modification of Mg_2X (X: Si, Sn) thermoelectric materials due to scandium addition

Cite as: J. Appl. Phys. **125**, 225103 (2019); doi: 10.1063/1.5089720
Submitted: 22 January 2019 · Accepted: 16 May 2019 ·
Published Online: 11 June 2019

Aryan Sankhla,[1,a)] Mohammad Yasseri,[1,2] Hasbuna Kamila,[1] Eckhard Mueller,[1,2] and Johannes de Boor[1,a)]

AFFILIATIONS

[1]Institute of Materials Research, Linder Hoehe, German Aerospace Center (DLR), D-51170 Koeln, Germany
[2]Institute of Inorganic and Analytical Chemistry, Justus Liebig University of Giessen, D-35392 Giessen, Germany

Note: This paper is part of the special topic on Advanced Thermoelectrics.
[a)]**Authors to whom correspondence should be addressed:** Aryan.Sankhla@dlr.de and Johannes.deBoor@dlr.de

ABSTRACT

Modification of the electronic band structure via doping is an effective way to improve the thermoelectric properties of a material. Theoretical calculations from a previous study have predicted that Sc substitution on the Mg site in Mg_2X materials drastically increase their Seebeck coefficient. Herein, we experimentally studied the influence of scandium substitution on the thermoelectric properties of $Mg_2Si_{0.4}Sn_{0.6}$ and Mg_2Sn. We found that the thermoelectric properties of these materials are unaffected by Sc addition, and we did not find hints for a modification of the electronic band structure. The SEM-energy dispersive X-ray analysis revealed that the scandium does not substitute Mg but forms a secondary phase (Sc-Si) in $Mg_2Si_{0.4}Sn_{0.6}$ and remains inert in Mg_2Sn, respectively. Thus, this study proves that scandium is an ineffective dopant for Mg_2X materials.

INTRODUCTION

Solid state devices fabricated from thermoelectric materials, which use waste heat to generate electrical power, are an effective way to increase the energy efficiency of various micro-/macrodevices.[1] They are currently being utilized in the automotive industry.[2] Furthermore, thermoelectric generators serve as an energy source where usual electric power supply is impossible, such as in space-probes.[3] Significant progress has been made in the past two decades in increasing the thermoelectric efficiency. This progress is achieved by exploiting fundamental concepts such as electronic band structure modification (carrier pocket engineering, band convergence, and resonant dopant levels), the scattering of phonons at nano-/microscale, size effect/quantum confinement, and self-optimization of carrier concentration.[4–8] These modifications have been applied to various thermoelectric material classes including magnesium silicides and its solid solutions (Mg_2X; X: Si, Sn, and Ge).[9,10] This promising class of material is very attractive, comprising features that include precursor abundance, lightweight, high thermoelectric performance ($zT \sim 1.1$–1.5), and environmental compatibility. The common strategies to increase the performance of thermoelectric materials such as the optimization of dopant concentration, alloying, and synthesizing solid solutions resulting in mass fluctuation to lower the thermal conductivity have already been applied successfully.[11–13] Apart from them, there have been attempts to modify the band structure by introducing various impurity atoms, with the aim to increase the thermoelectric performance of these materials further. In the quest for suitable/novel dopants, different theoretical and experimental studies have been performed. However, the theoretical studies do not provide a complete picture until an experimental confirmation is achieved. A lot of work has been dedicated to the X site in Mg_2X materials; however, only few impurity elements have been tried on the Mg site. Zhang *et al.* doped Co on the Mg site in $Mg_2(Si_{0.3}Sn_{0.7})_{1-y}Sb_y$ which resulted in the formation of CoSi as a secondary phase and

the samples behaved as intrinsic semiconductors.[14] Similarly, Sakamoto *et al.* and Zhao attempted doping Al, Cu, and Zn on the magnesium site in Mg_2Si materials, respectively.[14,15] Meng *et al.* doped yttrium (Y) possibly on the Mg site to observe an enhancement in the thermoelectric properties.[16] However, most of the previous studies did not give a clear picture on the influence of dopant substitution on the thermoelectric properties of the Mg_2X material (s). This is because often the dopant(s) tend(s) to form secondary phase(s) in a matrix or their role as an impurity is not fully understood, as they are co-doped with other impurity atoms (usually Sb or Bi). The notion of band structure modification and, in particular, resonant states in thermoelectric materials to increase their efficiency was introduced in the last decade.[17,18] Since then, several research groups have succeeded in exploiting this concept by the introduction of suitable dopants such as Tl in PbTe, Al in PbSe, V in $Hf_{0.75}Zr_{0.25}NiSn$, and recently Sn in As_2Te_3.[18–21] Bourgeois *et al.* reported in a density functional theoretical (DFT) study that transition metals could be prospective dopants on the Mg site. In particular, scandium (Sc) substitution could cause a shift in the Fermi level toward the conduction band and modify the density of states near the Fermi level, resulting in an increase in the Seebeck coefficient.[22] Moreover, Meng *et al.* also attempted doping scandium in Mg_2Si but were unable to make a proper conclusion on the effect of Sc on the thermoelectric properties of Mg_2Si.[16] In this study, we present experimental results and discuss the implications of doping scandium on the magnesium site (tetrahedral sites) in Mg_2X based materials.

MATERIAL AND METHODS

The scandium doped solid solutions of magnesium tin silicide ($Mg_2Si_{0.4}Sn_{0.6}$) and binary magnesium stannide (Mg_2Sn) were synthesized using commercially available starting elements [Mg turnings (Merck), Si (<6 mm, Chempure), Sn (<71 μm, Merck), Sc pieces (Chempure), and Sb (5 mm, Alfa Aesar)], all with purity >99.5%. A high energy ball mill (SPEX 8000D Shaker Mill) was used with stainless steel vials and balls. The elements were weighed according to the desired compositions with stoichiometries $Sc_xMg_{2-x}Si_{0.4}Sn_{0.6}$, $Sc_xMg_{2-x}Sn$ (x = 0.01, 0.05) and $Sc_xMg_{2.06-x}Sn_{1-y}Sb_y$ (x = 0.05, y = 0.03), respectively. The elemental precursors of $Sc_xMg_{2-x}Si_{0.4}Sn_{0.6}$ were mechanically alloyed for 20 h and 12 h for $Sc_xMg_{2-x}Sn$ and $Sc_xMg_{2.06-x}Sn_{1-y}Sb_y$ compositions, respectively. The powder handling during the synthesis was done under argon (Glove box; MBraun MB200) to prevent oxidation and contamination. The temperature/holding time to sinter the powder samples was 973 K/20 min for $Sc_xMg_{2-x}Si_{0.4}Sn_{0.6}$ samples and 873 K/10 min. for $Sc_xMg_{2-x}Sn$ and $Sc_xMg_{2.06-x}Sn_{1-y}Sb_y$ samples, respectively. A systematic study of optimal sintering temperature vs Si:Sn content can be found in Ref. 23. The powder samples were sintered by a direct-current sintering press (DSP 510 SE) from Dr. Fritsch GmbH. The sintering was performed using a graphite mold Ø12.7 mm under vacuum ($\sim 10^{-5}$ bar) at a heating rate of 1 K s^{-1}. The density of the compacted samples was measured using Archimedes' method. The relative densities of the pellets were >95% of the theoretical values ($Mg_2Si_{0.4}Sn_{0.6}$: 3.06 g cm^{-3} and Mg_2Sn: 3.59 g cm^{-3}), respectively. The XRD measurements on the samples were done utilizing a Siemens D5000 Bragg-Brentano diffractometer with a secondary monochromator. The parameters used were CuK_α radiation (1.5406 Å) in the 2θ range 20°–80° with a step size of 0.01°. The SEM analysis was done by a Zeiss Ultra 55 system equipped with an energy dispersive X-ray (EDS) detector. Moreover, the temperature dependent electronic properties were measured utilizing an in-house developed facility utilizing a four-probe technique.[24,25] The thermal diffusivity (α) of the pellets was obtained using a Netzsch LFA 467HT apparatus. The thermal conductivity (κ) was obtained using the relation $\kappa = \alpha\rho C_P$, where ρ and C_P are sample density and heat capacity, respectively. The C_P value was obtained from the Dulong-Petit limit for c_V^{DP}: $C_p = c_V^{DP} + \frac{9E_t^2T}{\beta_T\rho}$, $E_t^{Mg_2Si_{0.4}Sn_{0.6}} \sim 1.7 \times 10^{-5}\,K^{-1}$ and $\beta_T^{Mg_2Si_{0.4}Sn_{0.6}} \sim 2.07 \times 10^{-11}\,Pa^{-1}$, and $E_t^{Mg_2Sn} \sim 2.97 \times 10^{-5}\,K^{-1}$ and $\beta_T^{Mg_2Sn} \sim 2.4 \times 10^{-11}\,Pa^{-1}$ are the linear coefficient of thermal expansion and the isothermal compressibility for $Mg_2Si_{0.4}Sn_{0.6}$ and Mg_2Sn, respectively.[26,27] We found that the samples doped with Sc were more fragile than samples without Sc. The measurement error uncertainties for S, σ, and κ are ±5%, ±5%, and ±8%, respectively. The error bars are shown for one sample only for better visibility of the thermoelectric data. The room temperature Hall coefficient (R_H) of different samples was determined using an in-house facility in a van der Pauw configuration under a varying magnetic field of maximum $\pm 0.5\,T$. The Hall carrier concentration n_H was estimated from R_H assuming a single carrier type. The measurement uncertainties for n_H are ±10%.

RESULTS

The $Sc_{0.01}Mg_{1.99}Si_{0.4}Sn_{0.6}$ and $Sc_{0.05}Mg_{1.95}Si_{0.4}Sn_{0.6}$ samples are phase pure XRD-wise with no presence of secondary phases. The diffractograms of these samples were indexed by the ICSD standard pattern for $Mg_2Si_{0.4}Sn_{0.6}$ (ICSD PDF number 01-089-4254) confirming the formation of the desired phase (fcc, space group $Fm\bar{3}m$) [Fig. 1(a)]. The $Sc_{0.01}Mg_{1.99}Sn$, $Sc_{0.05}Mg_{1.95}Sn$, and $Sc_{0.05}Mg_{2.01}Sn_{0.97}Sb_{0.03}$ samples were indexed by the ICSD standard pattern for Mg_2Sn (ICSD PDF number 01-071-9596 65-2997) Fig. 1(b). The main phase was determined to be Mg_2Sn with the presence of elemental peaks of Sn and some peaks of scandium stannide phases (Sc_5Sn_3 and $ScSn_2$) in the XRD patterns of $Sc_{0.01}Mg_{1.99}Sn$, $Sc_{0.05}Mg_{1.95}Sn$, and $Sc_{0.05}Mg_{2.01}Sn_{0.97}Sb_{0.03}$ samples, respectively.

We have tabulated the lattice constants (Table I) of the $Mg_2Si_{0.4}Sn_{0.6}$ and Mg_2Sn samples doped with scandium. We find no change in the values of the lattice constants with increasing dopant concentration. The constant lattice parameter suggests no dopant incorporation to the parent compound.

EDS mappings were performed on the samples with compositions $Sc_{0.05}Mg_{1.95}Si_{0.4}Sn_{0.6}$ and $Sc_{0.05}Mg_{1.95}Sn$ as shown in Fig. 2. In Fig. 2(a), it is observed that the scandium in the sample reacts with silicon to form a Sc-Si based the secondary phase. In the latter sample, the scandium largely remains unreacted as an elemental impurity, as seen in Fig. 2(b). Moreover, the EDS point analysis on the $Sc_{0.05}Mg_{1.95}Sn$ sample revealed the presence of $ScSn_2$ islands which agree with the XRD pattern. For both sample types, Sc is thus observed only outside of the matrix phase. This is in agreement with the constancy of the lattice constant vs Sc content. Moreover, the secondary phase present in $Sc_{0.05}Mg_{1.95}Si_{0.4}Sn_{0.6}$ and $Sc_{0.05}Mg_{1.95}Sn$ was determined by the backscattered image contrast, and area-wise quantified to be 2.2% and 1.4%, respectively.[28]

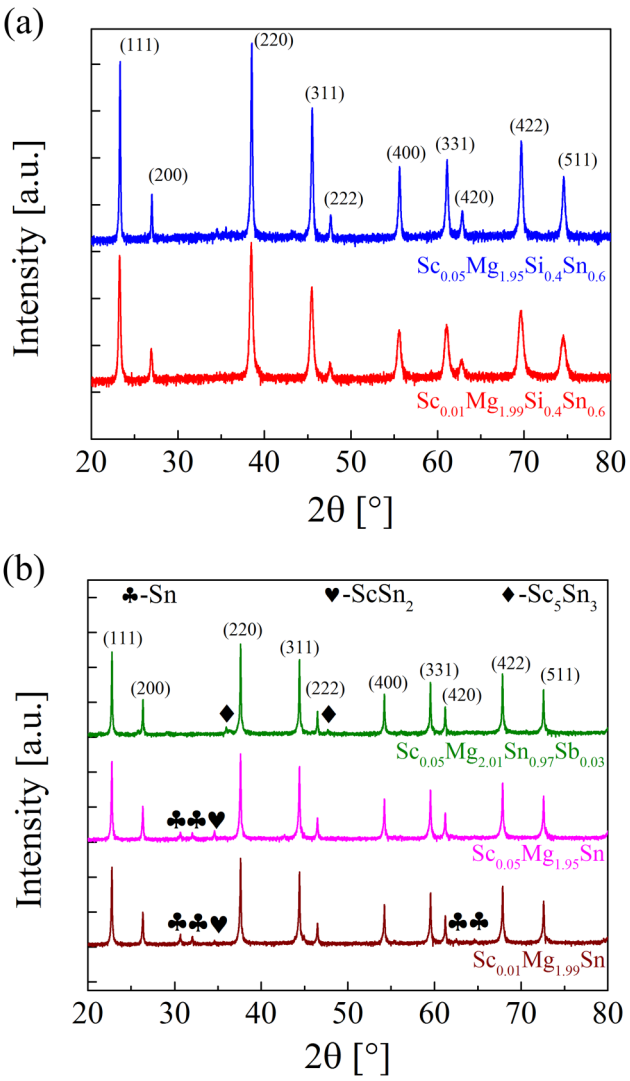

FIG. 1. XRD patterns of (a) $Sc_{0.01}Mg_{1.99}Si_{0.4}Sn_{0.6}$ and $Sc_{0.05}Mg_{1.95}Si_{0.4}Sn_{0.6}$ and (b) $Sc_{0.01}Mg_{1.99}Sn$, $Sc_{0.05}Mg_{1.95}Sn$, and $Sc_{0.05}Mg_{2.01}Sn_{0.97}Sb_{0.03}$ samples.

TABLE I. List of sample compositions, their lattice constants, and relative sample densities.

Composition	Lattice constant (Å)	Relative sample density (%)
$Sc_{0.01}Mg_{1.99}Si_{0.4}Sn_{0.6}$	6.528	97.8
$Sc_{0.05}Mg_{1.95}Si_{0.4}Sn_{0.6}$	6.528	98.4
$Sc_{0.01}Mg_{1.99}Sn$	6.692	98.6
$Sc_{0.05}Mg_{1.95}Sn$	6.692	100.8
$Sc_{0.05}Mg_{2.01}Sn_{0.97}Sb_{0.03}$	6.692	97.7

The temperature dependence of Seebeck coefficient and electrical conductivity data for all the samples shown in Fig. 3 follows the trend corresponding to an intrinsic semiconductor. We observe a slight lowering of the Seebeck coefficient with an increase in dopant concentration and a subtle increase in the electrical conductivity near room temperature. The change in Seebeck coefficient/electrical conductivity near room temperature could be possibly due to the presence of secondary phases, as observed from the SEM/EDS data (as both Sc_5Si_3 and ScSi have quite high electrical conductivity[29]).

We observe from Fig. 3(c) that the thermal conductivity for all the samples shows a similar trend with first a decrease with temperature and then an increase due to the bipolar effect of intrinsic charge carriers at temperatures around 500 K. Mainly as a result of the increased electrical conductivity, the zT_{max} (~0.19) values get almost doubled with an increase of Sc concentration in $Sc_xMg_{2-x}Si_{0.4}Sn_{0.6}$.

As observed from the SEM, the formation of scandium silicide secondary phase in $Sc_{0.05}Mg_{1.95}Si_{0.4}Sn_{0.6}$ prevented an evaluation of the influence of scandium in the parent compound. The Si-Sc phase diagram points out that there could be a formation of Sc_5Si_3 and ScSi phases for Si-Sc.[30] Thus, to observe an effect of scandium on the thermoelectric properties of Mg_2X materials, we investigated the binary Mg_2Sn compound and doped it with different concentrations of scandium. The temperature dependent transport data can be observed from Fig. 4. It can be seen that the undoped sample has a positive Seebeck coefficient at room temperature, while the samples with Sc exhibit a negative Seebeck coefficient. This, together with the temperature dependence of the electrical conductivity, indicates that all three samples have mixed conduction with the Sc samples having a higher number of electrons. This could be due to very inefficient doping of Sc or due to a change of the intrinsic defect concentrations, induced by the addition of Sc or the change in Sc:Mg ratio.[10] In order to check for any modification of the electronic band structure of Sc (even if not acting as an efficient dopant), we co-doped the 2.5% Sc-doped Mg_2Sn sample with 3% Sb and compared it with the 3% Sb-doped Mg_2Sn sample. The electronic transport properties for both of these samples were found to be almost identical. This suggests that there is no influence of Sc doping on the thermoelectric properties of Mg_2X based materials. Thus, this experimental observation contradicts the theoretical work on Mg_2X claiming Sc being a prospective dopant.[22] We utilized high energy ball milling as the synthesis technique for $Mg_2(Si,Sn)$ and Mg_2Sn, which is known for its high dopant efficiency in comparison to other techniques.[11,31]

DISCUSSION

The band structure simulations for scandium doped Mg_2X materials suggest that scandium (Sc) is a potential dopant. However, taking other aspects into account such as formation enthalpies, phase diagram analysis, etc., it is observed that for Sc-doped $Mg_2(Si,Sn)$ materials, scandium favorably reacts with silicon rather than substituting magnesium. This is in accordance with quite high formation enthalpies of ScSi [-117.2 kJ mol^{-1} (at 298 K) and -87.1 ± 2.1 kJ mol^{-1} (825–1045 K)] and of Sc_5Si_3 [-161.1 kJ mol^{-1} (at 298 K) and -102.8 ± 3.2 kJ mol^{-1} (835–895 K)].[32]

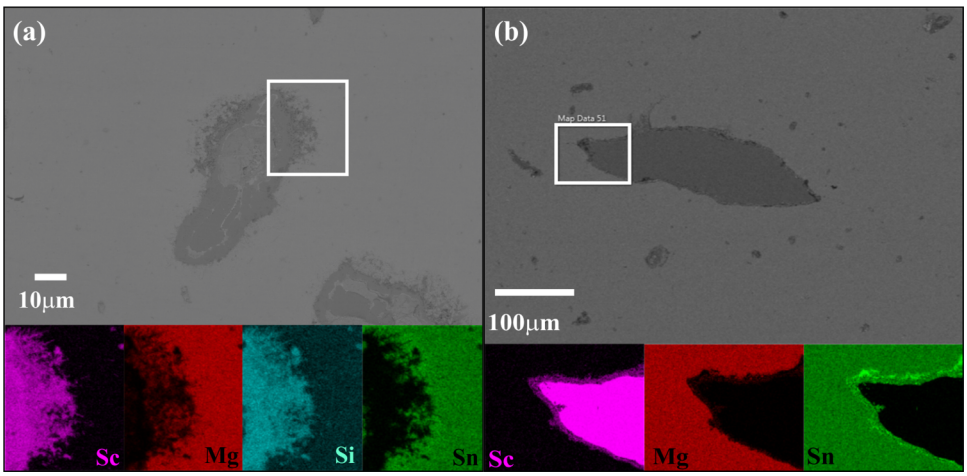

FIG. 2. EDS mapping on (a) $Sc_{0.05}Mg_{1.95}Si_{0.4}Sn_{0.6}$ and (b) $Sc_{0.05}Mg_{1.95}Sn$ samples. In the sample with composition $Sc_{0.05}Mg_{1.95}Si_{0.4}Sn_{0.6}$, a region with the presence of scandium and silicon can be seen clearly. On further point analysis, it reveals a composition close to Sc_5Si_3 and some excess unreacted silicon. In the sample with composition $Sc_{0.05}Mg_{1.95}Sn$, scandium stays unreacted and can be observed as a secondary phase.

This also suggests that the formed Sc-Si phase would probably be Sc_5Si_3.[30] Qualitatively, the Sc-Si phases have a higher room temperature electrical conductivity values than Mg_2X materials which possibly explains the subtle variations in the properties at near room temperature of Sc-doped $Mg_2Si_{0.4}Sn_{0.6}$ materials.[29] However, this cannot be quantified since these secondary phases are not present continuously throughout the samples. We doped binary Mg_2Sn (without Si) with Sc to avoid the formation of scandium silicide phase as in $Mg_2(Si,Sn)$. Even though the Sn-Sc phase diagram indicates the existence of Sc_5Sn_3 and $ScSn_2$ phases, these phases have lower formation energy (Sc_5Sn_3: $-56.04\ kJ\ mol^{-1}$ and $ScSn_2$: $-44.9\ kJ\ mol^{-1}$)[33] than Sc-Si phases. Therefore, it was previously unclear whether scandium substitutes Mg in Mg_2Sn, forms a Sn-Sc secondary phase or remains inert. The $Sc_xMg_{2-x}Sn$ samples

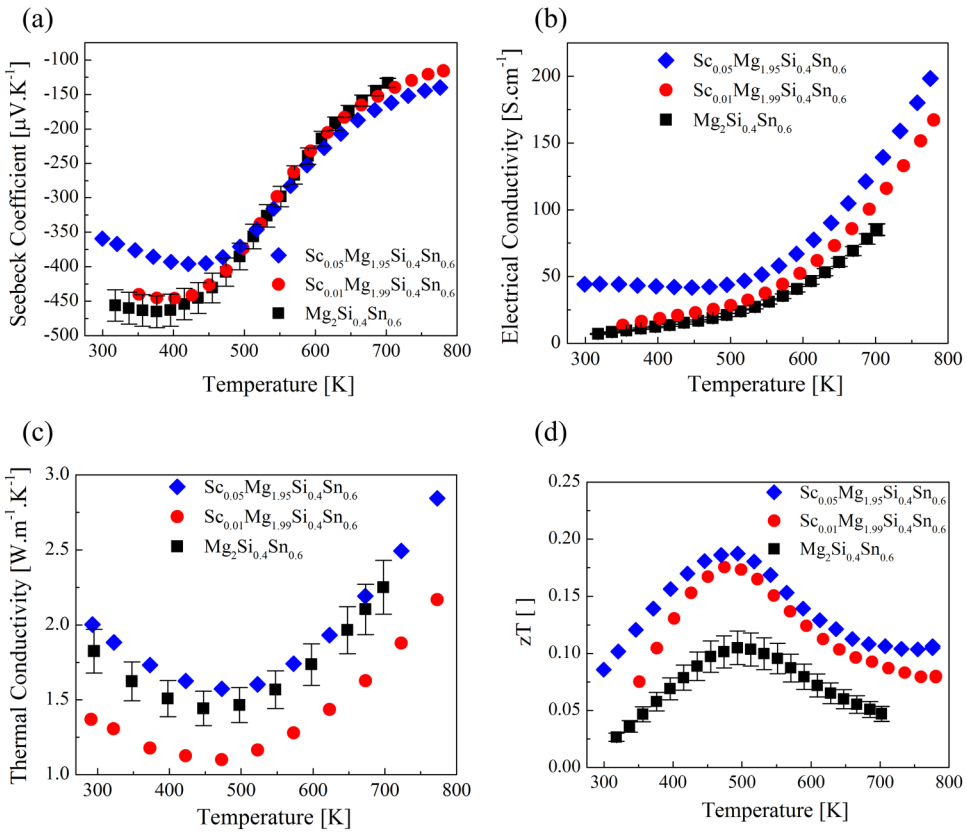

FIG. 3. Temperature dependent (a) Seebeck coefficient, (b) electrical conductivity, (c) thermal conductivity, and (d) figure-of-merit (zT) of undoped, $Sc_{0.01}Mg_{1.99}Si_{0.4}Sn_{0.6}$, and $Sc_{0.05}Mg_{1.95}Si_{0.4}Sn_{0.6}$ samples.

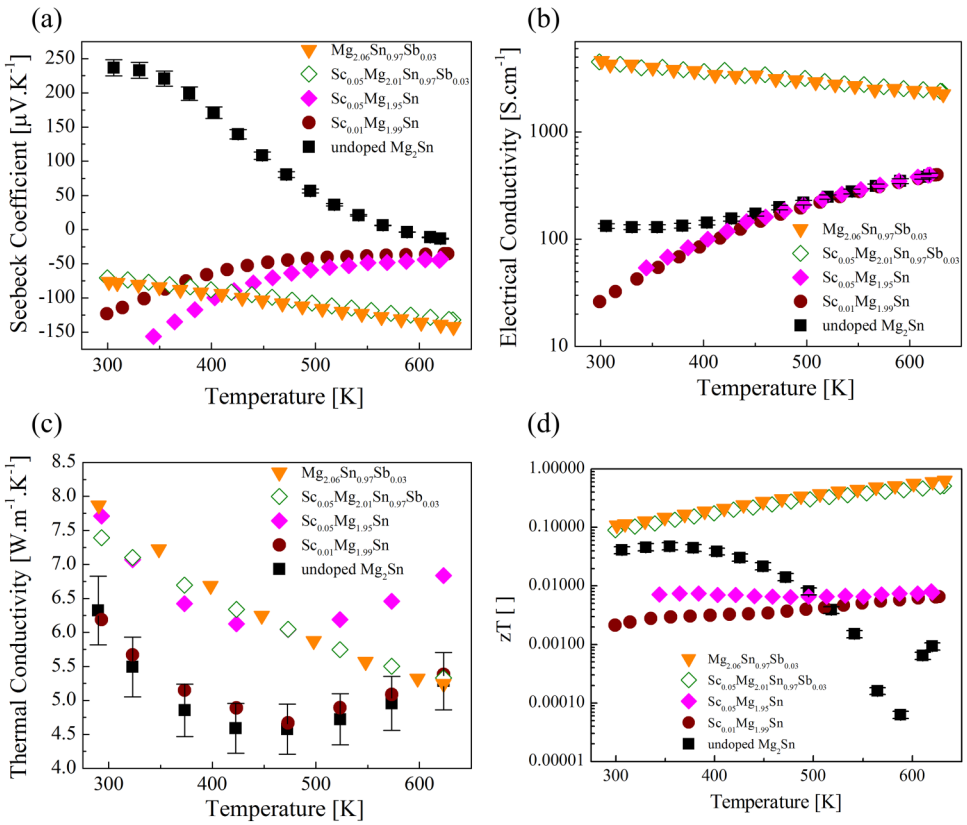

FIG. 4. Temperature dependent (a) Seebeck coefficient, (b) electrical conductivity, (c) thermal conductivity, and (d) figure-of-merit (zT) of undoped, $Sc_{0.01}Mg_{1.99}Sn$, $Sc_{0.05}Mg_{1.95}Sn$, $Sc_{0.05}Mg_{2.01}Sn_{0.97}Sb_{0.03}$, and $Mg_{2.06}Sn_{0.97}Sb_{0.03}$ samples, respectively. The Y-axis of the electrical conductivity and estimated zT plots has a logarithmic scale for better visualization of the data.

show a weak n-type character at room temperature. This n-type character of the samples could possibly be a result of either elemental Sc that has a Seebeck coefficient between −6 and $-10\,\mu V\,K^{-1}$[34,35] or due to a change in the intrinsic defect concentration that leads to a change in character from a p-type to an n-type material. A similar effect was observed by Liu *et al.* in their study on the Ga doping in p-type $Mg_2Si_{0.3}Sn_{0.7}$ material.[36] This weak n-type nature of these samples can be a combination of both the aforementioned effects. We also carried out room temperature Hall measurements (n_H) on both Sc-doped $Mg_2Si_{0.4}Sn_{0.6}$ and Sc-doped Mg_2Sn samples to observe an effect of scandium addition to the stoichiometry. The values are tabulated in Table II. However, we found negligible change to the magnitude of n_H for these "doped" samples in comparison with the carrier concentration of their respective undoped samples. The $Sc_{0.05}Mg_{2.01}Sn_{0.97}Sb_{0.03}$ sample showed poor mechanical strength and the Hall measurement was, therefore, not feasible on this sample. We estimated n_H for this sample from the Seebeck coefficient by employing a single parabolic band (SPB) model in the following manner. First, we obtained a density-of-states effective mass $m_D^*=2.0m_0$ for $Mg_{2.06}Sn_{0.97}Sb_{0.03}$ using the experimental value of the Seebeck coefficient to obtain the reduced chemical potential η from $S=\frac{k}{e}\left(\frac{2F_1(\eta)}{F_0(\eta)}-\eta\right)$ and then m_D^* was obtained from $n=4\pi\left(\frac{2m_D^*k_BT}{h^2}\right)^{\frac{3}{2}}F_{0.5}(\eta)$. $F_j(\eta)$ are the Fermi integrals and n is related to the experimentally obtained Hall carrier concentration n_H by $n=n_H.r_H$ with $r_H=\frac{3}{2}.F_{0.5}(\eta)\frac{F_{-0.5}(\eta)}{2F_0^2(\eta)}$. These equations assume an SPB with mobility limited by acoustic phonon scattering [scattering parameter ($\lambda=0$)]. Finally, the obtained value of $m_D^*=2.0m_0$ was used to estimate n of $Sc_{0.05}Mg_{2.01}Sn_{0.97}Sb_{0.03}$ from the measured S value and the above equations.

TABLE II. Sample compositions, Seebeck coefficient at room temperature, theoretical carrier concentration, and Hall carrier concentration of scandium and antimony doped Mg_2X (X: Si, Sn) samples. The value marked with an asterisk was estimated using a single parabolic band model using the room temperature Seebeck coefficient values of that sample.

Composition	Seebeck coefficient ($\mu V\,K^{-1}$)	Theoretical n ($\times10^{19}$) (cm^{-3})	n_H ($\times10^{19}$) (cm^{-3})
$Mg_2Si_{0.4}Sn_{0.6}$			
Undoped $Mg_2Si_{0.4}Sn_{0.6}$	−425	…	0.2
$Sc_{0.01}Mg_{1.99}Si_{0.4}Sn_{0.6}$	−401	14.3	0.22
$Sc_{0.05}Mg_{1.95}Si_{0.4}Sn_{0.6}$	−343	71.8	0.56
Mg_2Sn			
Undoped Mg_2Sn	243	…	0.57
$Sc_{0.01}Mg_{1.99}Sn$	−125	13.3	0.59
$Sc_{0.05}Mg_{1.95}Sn$	−218	66.7	0.47
$Sc_{0.05}Mg_{2.01}Sn_{0.97}Sb_{0.03}$	−69	107	44*
$Mg_{2.06}Sn_{0.97}Sb_{0.03}$	−74	39	38

The theoretical carrier concentration was calculated assuming that one scandium atom substitutes one magnesium atom and one antimony atom substitutes one tin atom in the lattice of the complete crystal of the compound(s), respectively, both effectively providing one additional electron. The total number of atoms in a crystal was estimated from the lattice constant corresponding to the most significant peak in the XRD pattern of each sample. The theoretical carrier concentration of $Mg_{2.06}Sn_{0.97}Sb_{0.03}$ sample was estimated using the literature values of the lattice constant for Mg_2Sn.[37] Thus, the Hall measurements confirm no influence of scandium substitution.

On the other hand, the thermal conductivity of $Sc_xMg_{2-x}Sn$ (x: 0.01 and 0.05) samples show a difference of ~15%–18%, with $Sc_{0.05}Mg_{1.95}Sn$ having higher room temperature values. This could be qualitatively understood from the XRD and the EDS data of $Sc_{0.05}Mg_{1.95}Sn$ sample that has a higher Sc content as a secondary phase than Mg_2Sn[38] and $Sc_{0.01}Mg_{1.99}Sn$. However, zT is not affected much and has a value of ~0.008 for $Sc_{0.05}Mg_{1.95}Sn$.

CONCLUSION

In this study, we have investigated the effect of scandium doping on Mg_2X thermoelectric materials. The presence of secondary phases was ascertained by EDS analysis on scanning electron micrographs of the samples. These EDS mappings reveal that elemental scandium forms an Sc-Si phase when added to $Mg_2Si_{0.4}Sn_{0.6}$ and remains mostly unreacted in Mg_2Sn samples. The thermoelectric data suggest that scandium in $Mg_2Si_{0.4}Sn_{0.6}$ does not act as a dopant. The zT value for $Sc_{0.05}Mg_{1.95}Si_{0.4}Sn_{0.6}$ was $zT_{max} \sim 0.19$. An addition of Sc to Mg_2Sn samples turns the samples into n-type, but the carrier concentration remains far below the optimum range. The thermoelectric properties of Sb-doped and Sb, Sc co-doped samples reveal no significant difference on comparison. Thus, the current study strongly suggests that Sc is not a suitable dopant for Mg_2X materials.

ACKNOWLEDGMENTS

We would like to gratefully acknowledge the endorsement from DLR Executive Board Members for Space Research and Technology and the financial support from Young Research Group Leader Program. The authors would like to thank P. Blaschkewitz (DLR) for his untiring support with the thermoelectric measurements. The authors (A.S. and H.K.) would like to acknowledge financial support by the DAAD (Fellowship No. 247). Also, financial support of one of the authors (M.Y.) is provided by the DFG via the GRK (Research Training Group) 2204 "Substitute Materials for Sustainable Energy Technologies."

REFERENCES

[1]G. J. Snyder and E. S. Toberer, Nat. Mater. **7**, 105 (2008).
[2]X. Liu, Y. D. Deng, Z. Li, and C. Q. Su, Energy Convers. Manage. **90**, 121 (2015).
[3]T. M. Tritt and M. A. Subramanian, MRS Bull. **31**, 188 (2006).
[4]J. Mao, Z. Liu, and Z. Ren, npj Quantum Mater. **1**, 16028 (2016).
[5]W. Liu, X. Tan, K. Yin, H. Liu, X. Tang, J. Shi, Q. Zhang, and C. Uher, Phys. Rev. Lett. **108**, 166601 (2012).
[6]K. Biswas, J. He, I. D. Blum, C.-I. Wu, T. P. Hogan, D. N. Seidman, V. P. Dravid, and M. G. Kanatzidis, Nature **489**, 414 (2012).
[7]Y. Pei, A. F. May, and G. J. Snyder, Adv. Energy Mater. **1**, 291 (2011).
[8]J. P. Heremans, B. Wiendlocha, and A. M. Chamoire, Energy Environ. Sci. **5**, 5510 (2012).
[9]J. de Boor, T. Dasgupta, U. Saparamadu, E. Müller, and Z. F. Ren, Mater. Today Energy **4**, 105 (2017).
[10]X. Liu, L. Xi, W. Qiu, J. Yang, T. Zhu, X. Zhao, and W. Zhang, Adv. Electron. Mater. **2**, 1500284 (2016).
[11]A. Sankhla, A. Patil, H. Kamila, M. Yasseri, N. Farahi, E. Mueller, and J. de Boor, ACS Appl. Energy Mater. **1**, 531 (2018).
[12]P. Gao, I. Berkun, R. D. Schmidt, M. F. Luzenski, X. Lu, P. Bordon Sarac, E. D. Case, and T. P. Hogan, J. Electron. Mater. **43**, 1790 (2014).
[13]N. Farahi, S. Prabhudev, G. A. Botton, J. R. Salvador, and H. Kleinke, ACS Appl. Mater. Interfaces **8**, 34431 (2016).
[14]Q. Zhang, W. Liu, C. Liu, K. Yin, and X. F. Tang, J. Electron. Mater. **43**, 2188 (2014).
[15]T. Sakamoto, T. Iida, A. Matsumoto, Y. Honda, T. Nemoto, J. Sato, T. Nakajima, H. Taguchi, and Y. Takanashi, J. Electron. Mater. **39**, 1708 (2010).
[16]Q. S. Meng, W. H. Fan, R. X. Chen, and Z. A. Munir, J. Alloys Compd. **509**, 7922 (2011).
[17]D. Bilc, S. D. Mahanti, E. Quarez, K.-F. Hsu, R. Pcionek, and M. G. Kanatzidis, Phys. Rev. Lett. **93**, 146403 (2004).
[18]J. P. Heremans, V. Jovovic, E. S. Toberer, A. Saramat, K. Kurosaki, A. Charoenphakdee, S. Yamanaka, and G. J. Snyder, Science **321**, 554 (2008).
[19]J. W. Simonson, D. Wu, W. J. Xie, T. M. Tritt, and S. J. Poon, Phys. Rev. B **83**, 235211 (2011).
[20]B. Wiendlocha, J.-B. Vaney, C. Candolfi, A. Dauscher, B. Lenoir, and J. Tobola, Phys. Chem. Chem. Phys. **20**, 12948 (2018).
[21]Q. Zhang, H. Wang, W. Liu, H. Wang, B. Yu, Q. Zhang, Z. Tian, G. Ni, S. Lee, K. Esfarjani, G. Chen, and Z. Ren, Energy Environ. Sci. **5**, 5246 (2012).
[22]J. Bourgeois, J. Tobola, B. Wiendlocha, L. Chaput, P. Zwolenski, D. Berthebaud, F. Gascoin, Q. Recour, and H. Scherrer, Funct. Mater. Lett. **06**, 1340005 (2013).
[23]H. Kamila, A. Sankhla, M. Yasseri, N. P. Hoang, N. Farahi, E. Mueller, and J. de Boor, Mater. Today Proc. **8**, 546 (2019).
[24]J. D. Boor and E. Müller, Rev. Sci. Instrum. **84**, 065102 (2013).
[25]J. de Boor, C. Stiewe, P. Ziolkowski, T. Dasgupta, G. Karpinski, E. Lenz, F. Edler, and E. Mueller, J. Electron. Mater. **42**, 1711 (2013).
[26]K. A. Borup, J. de Boor, H. Wang, F. Drymiotis, F. Gascoin, X. Shi, L. Chen, M. I. Fedorov, E. Müller, B. B. Iversen, and G. J. Snyder, Energy Environ. Sci. **8**, 423 (2015).
[27]*Non-Tetrahedrally Bonded Elements and Binary Compounds I*, edited by O. Madelung, U. Rössler, and M. Schulz (Springer, Berlin, 1998), p. 1.
[28]M. Yasseri, N. Farahi, K. Kelm, E. Mueller, and J. de Boor, Materialia **2**, 98–103 (2018).
[29]O. Thomas, C. S. Petersson, and F. M. d'Heurle, Appl. Surf. Sci. **53**, 138 (1991).
[30]H. Okamoto, J. Phase Equilib. **13**, 679 (1992).
[31]J. Mao, H. S. Kim, J. Shuai, Z. Liu, R. He, U. Saparamadu, F. Tian, W. Liu, and Z. Ren, Acta Mater. **103**, 633 (2016).
[32]G. M. Lukashenko, R. I. Polotskaya, and V. R. Sidorko, J. Alloys Compd. **179**, 299 (1992).
[33]A. Iddaoudi, N. Selhaoui, M. Ait Amar, S. Kardellass, R. Karioui, and L. Bouirden, Calphad **41**, 71 (2013).
[34]M. V. Vedernikov, Adv. Phys. **18**, 337 (1969).
[35]N. V. Morozova, V. V. Shchennikov, and S. V. Ovsyannikov, J. Appl. Phys. **118**, 225901 (2015).
[36]W. Liu, K. Yin, X. Su, H. Li, Y. Yan, X. Tang, and C. Uher, Intermetallics **32**, 352 (2013).
[37]H. Kasai, L. Song, H. L. Andersen, H. Yin, and B. B. Iversen, Acta Crystallogr. Sect. B **73**, 1158 (2017).
[38]B. W. Jolliffe, R. P. Tye, and R. W. Powell, J. Less Common Met. **11**, 388 (1966).